Available online at www.sciencedirect.com
ScienceDirect
Ceramics International 38S (2012) S595–S599
CERAMICS INTERNATIONAL
www.elsevier.com/locate/ceramint

Relationships between the crystalline phase of an IGZO target and electrical properties of a-IGZO channel film

Yih-Shing Lee [a,*], Zuo-Ming Dai [b], Cheng-I Lin [c], Horng-Chih Lin [c]

[a] Department of Optoelectronic System Engineering, Minghsin University of Science and Technology, Hsin-Fong, Hsin-Chu 30401, Taiwan, ROC
[b] Institute of Electronics, Minghsin University of Science and Technology, Hsin-Chu 30401, Taiwan, ROC
[c] Institute of Electronics and Department of Electronic Engineering, National Chiao Tung University, Hsin-Chu 300, Taiwan, ROC

Available online 27 May 2011

Abstract

This study used powders containing different In_2O_3–Ga_2O_3–ZnO (IGZO) chemical compositions to manufacture targets using a metallurgical process. The resulting targets were used to deposit amorphous In–Ga–Zn–O (a-IGZO) channel films by a radio frequency magnetron sputtering process. This study examined the relationships between these target compositions and crystalline phases of the powders and the resulting material characterization, examining the impacts on electrical characteristics of a-IGZO films with varied O_2 flow rates. The ternary compound phase of $ZnGa_2O_4$ became stable at 1000 °C according to XRD diagrams at different calcining temperatures. An analysis of the XRD diagrams of different compositions of IGZO powders showed that the atomic ratio of ZnO is larger than that of In_2O_3 and Ga_2O_3, and that the main peaks (1 0 1) and (0 0 15) intensity of the respective $InGaZnO_4$ and $InGaZnO_6$ phases intensity would increase. Ceramic targets with different compositions were used to deposit the a-IGZO films with varied O_2 flow rates. When the O_2 flow rate was zero, the results of a Hall measurement of a-IGZO films deposited from targets with higher Zn atomic ratio showed lower resistivity, higher carrier concentration, and lower mobility. Nevertheless, as the O_2 flow rate was more than 5 sccm, increasing the atom ratio of Zn in the IGZO ceramic target obviously increased the capability of capturing O_2 in the a-IGZO films, leading to higher resistivity, lower carrier concentration ($<10^{18}$ cm^{-3}), and higher mobility.

Keywords: A. Films; B. X-ray methods; C. Electrical properties; IGZO

1. Introduction

Transparent amorphous oxide semiconductors (TAOSs) are promising for channel materials of thin-film transistors [1] (TFTs) and are used primarily for driving TFTs in organic light-emitting diode displays due to large mobilities (>10 cm^2 V^{-1} s^{-1}) and low process temperatures. Several TAOSs, such as amorphous In–Ga–Zn–O (a-IGZO) [1–3], In–Zn–O [4,5], Zn–Sn–O [6], and In–Sn–O [7], have been reported as channel materials of TFTs to date. As such, an essential feature of TAOSs is that they are multi-component materials, and, therefore have a large flexibility to tune properties for TFTs. However, this feature raises a problem in determining the optimal chemical composition and fabrication condition in such a large parameter space. Therefore, we require an efficient technique to survey systematically a material over a wide chemical composition and under deposition conditions for the active layers of the TFTs.

Moreover, the most vital characteristic for device applications is that the carrier concentration must be controlled at low levels, for example, $<10^{15}$ cm^{-3}, with favorable stability and reproducibility to control device characteristics, such as threshold voltage, and to suppress the off-current [3]. Powder targets degrade crystal growth quality of ZnO films; therefore, ceramic targets were prepared for a-IGZO film by an RF sputtering system [8]. This paper reports the relationships between the crystalline phases of different compositions of In_2O_3–Ga_2O_3–ZnO (IGZO) targets and the Hall electrical properties of a-IGZO channel film prepared by RF magnetron sputtering with varied O_2 flow rates.

2. Experimental procedure

The different composition of IGZO powder used in the experiment was mixed by the atomic ratios of In:Ga:Zn = 2:2:1,

* Corresponding author. Tel.: +886 3 5593142 3383; fax: +886 5593142 3388.
E-mail address: yslee@must.edu.tw (Y.-S. Lee).

0272-8842/$36.00
doi:10.1016/j.ceramint.2011.05.105

1:1:1, and 1:1:2. The powders were then milled, followed by calcining at various temperatures of 730, 930, and 1030 °C for 1 h, respectively. Next, the powders were ground, sieved through a 250-mesh screen, and were formed into the sputter target with the pressure of 60,000–70,000 kg/cm^2 at 1250 °C for 1 h in an Ar ambient. The a-IGZO films were deposited at room temperature using an RF magnetron sputtering system (LJUHV LJ-303CL) on the glass substrates of SCHOTT B270. In the deposition process, the sputtering power was set at 250 W and the working pressure was controlled at 5E − 3 Torr. Additionally, the sputtering conditions of a-IGZO film were set at the fixed Ar flow (50 sccm) with varied O_2 flow rates (0 sccm, 2 sccm, 5 sccm, 7 sccm, and 10 sccm). After deposition, the samples were annealed at 400 °C with 5E − 3 Torr working pressure for 1 h in N_2 ambient of 40 sccm.

The crystallinities of different IGZO powders were also analyzed by XRD (X-Ray diffraction) (PANalytical X'Pert Pro) with a Ni-filtered Cu Kα (λ = 1.5418 Å) source in θ–2θ scanning mode. The scanning angle was between 20° and 80°. Hall measurement was utilized with the van der Pauw method by using the HL5500PC (Bio-Rad). The magnetic field applied in the measurement was at 0.323 T. The test samples were cut into squares 1 cm^2. The film sheet resistance and thickness were measured by a 4-point probe (Napson RT-80) and an N&K1500, respectively.

3. Results and discussion

Fig. 1 shows XRD diagrams of IGZO1 (In_2O_3:Ga_2O_3:ZnO = 2:2:1) powders that were calcined at different temperatures of 730, 930, and 1030 °C for 1 h, respectively. Different phase orientations of In_2O_3 and $ZnGaO_4$ are indicated in Fig. 1. Beyond the calcinations temperature of 1000 °C, the main phase orientation (2 2 2) peak of In_2O_3 decreased, and those peaks (4 0 0), (5 1 1), and (4 4 0) intensity of $ZnGa_2O_4$ increased and saturated. This implied that the ternary compounds of $ZnGa_2O_4$ reacted completely and those peaks were similar with the XRD results of $ZnGa_2O_4$ targets, as measured according to Krishna et al. [9]. Fig. 2 shows XRD diagrams of IGZO powders with different atomic ratios of In:Ga:Zn calcined at 730 °C for 1 h. Different phase orientations of In_2O_3, $ZnGa_2O_4$, $InGaZnO_4$, and $InGaZnO_6$ are indicated in Fig. 2. When the atomic ratio of ZnO was larger than that of In_2O_3 and Ga_2O_3, the main peaks (1 0 1) and (0 0 15) intensity of the respective $InGaZnO_4$ and $InGaZnO_6$ phases intensity increased. Those peaks were also shown in the XRD patterns of the $InGaZnO_4$ target [10]. Nevertheless, the main peaks (2 2 2) and (3 1 1) intensity of the respective In_2O_3 and $ZnGa_2O_4$ phases decreased gradually as the ZnO atomic ratio increased.

Fig. 3 shows the Hall measurement plot of a-IGZO1 film (In:Ga:Zn = 2:2:1) as a function of O_2 flow rates with a fixed Ar flow, 50 sccm. The resistivity increased linearly with the O_2 flow rate first, and then reached saturation at the high O_2 flow rate [2,11]. By increasing the O_2 flow rate, the carrier concentration decreased at the lower O_2 flow rate (<5 sccm), sccm), but the carrier concentration increased at the high O_2 flow rate condition (>5 sccm). At the high O_2 flow rate condition (>5 sccm), the concentration and the mobility became a trade-off due to the scattering of the oxygen vacancy and whether the grain density was tight or not. Fig. 4 shows the SEM graphs for a-IGZO1 film with the deposition condition at

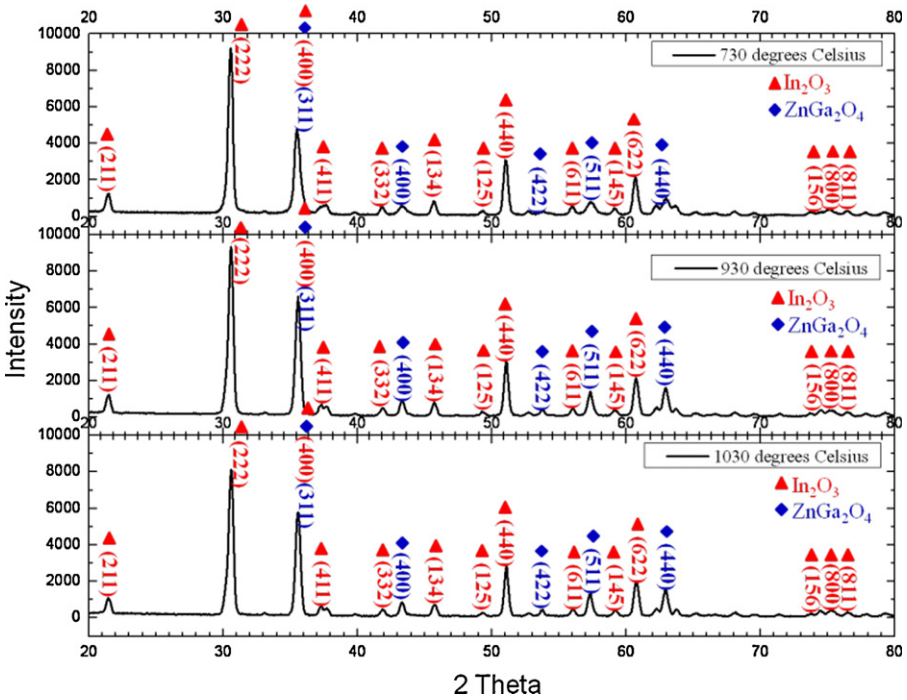

Fig. 1. XRD diagrams of IGZO1 (In_2O_3:Ga_2O_3:ZnO = 2:2:1) powders were calcined at different temperatures for 1 h, different phase orientations of In_2O_3 and $ZnGa_2O_4$ were indicated in the diagram.

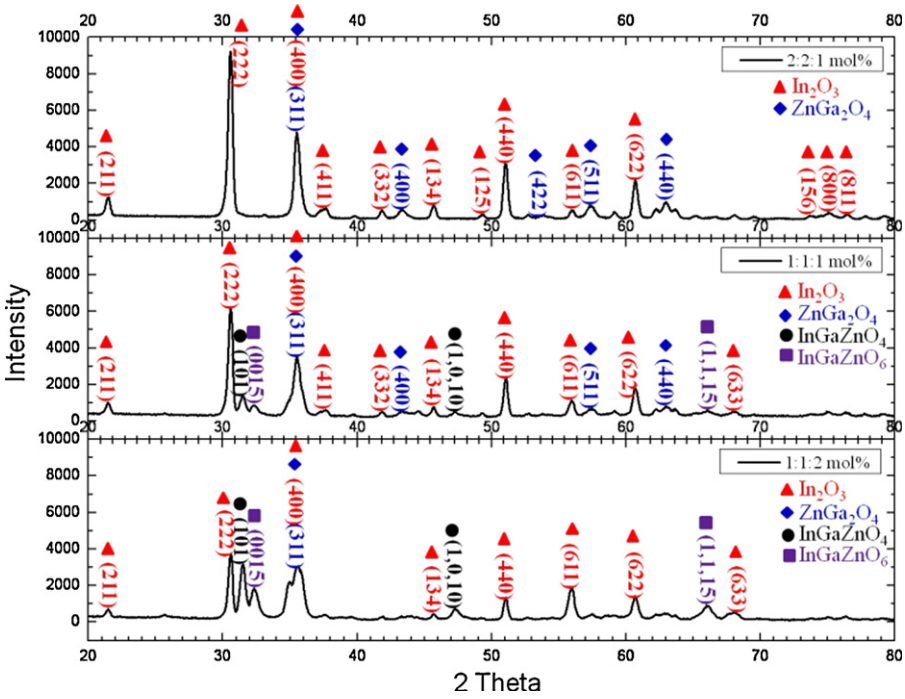

Fig. 2. XRD diagrams of IGZO powders with the different atomic ratios of In:Ga:Zn calcined at 730 °C for 1 h, different phase orientations of In_2O_3, $ZnGa_2O_4$, $InGaZnO_4$, and $InGaZnO_6$ were indicated in the diagram.

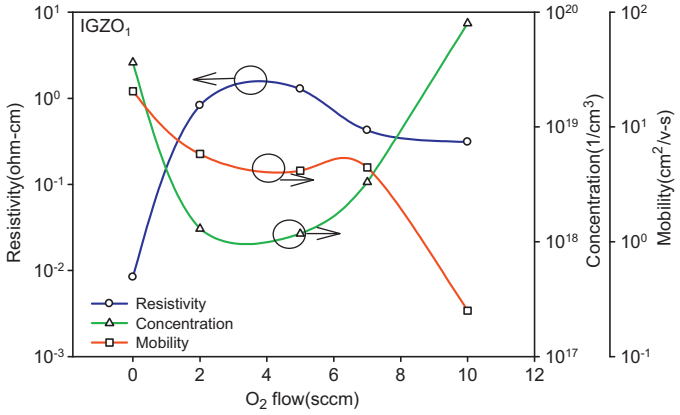

Fig. 3. Hall measurement plot of a-IGZO1 film (In:Ga:Zn = 2:2:1) as a function of O_2 flow rates with fixed Ar flow, 50 sccm.

O_2 flow at 0 and 2 sccm, respectively. It can be seen that the sample added element of O_2 appears looser in the film, ascribed to incomplete surface reaction in the film due to less content of Zn in the a-IGZO1 target. Less content of Zn decreases the capability of O_2 capture. Therefore, loose appearance in the surface indicates lower mobility. Fig. 5 shows the SEM graphs for a-IGZO2 film (In:Ga:Zn = 1:1:1) with the deposition condition at O_2 flow at 0 and 2 sccm, respectively. The result of a-IGZO3 (In:Ga:Zn = 1:1:2) is the same as that of a-IGZO2. Adequate content of Zn existed in the film; therefore, the capability of O_2 capture was promoted and the surface could react completely and display densely when the O_2 was added. Afterward, the mobility rose with the added O_2 flow. Fig. 6 shows the Hall measurement plot of a-IGZO2 film (In:Ga:Zn = 1:1:1) as a function of O_2 flow rates with a fixed Ar flow equal to 50 sccm. By increasing the O_2 flow rate, the carrier concentration first decreased at the lower O_2 flow rate (<5 sccm), then slightly increased at the higher O_2 flow rate

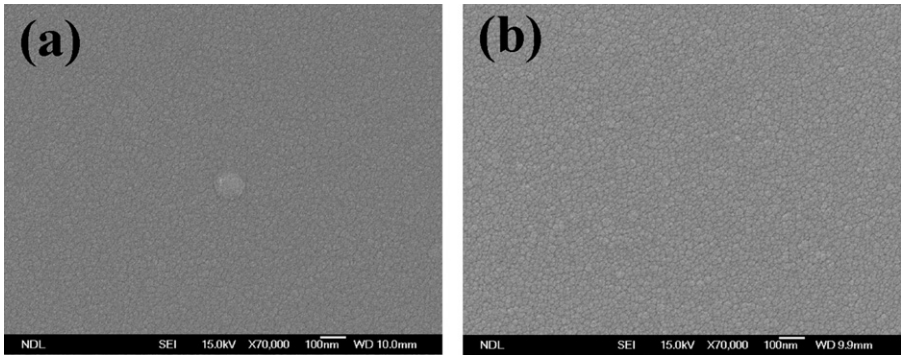

Fig. 4. SEM graphs of a-IGZO1 film (In:Ga:Zn = 2:2:1) with O_2 flow rates at (a) 0 and (b) 2 sccm, respectively.

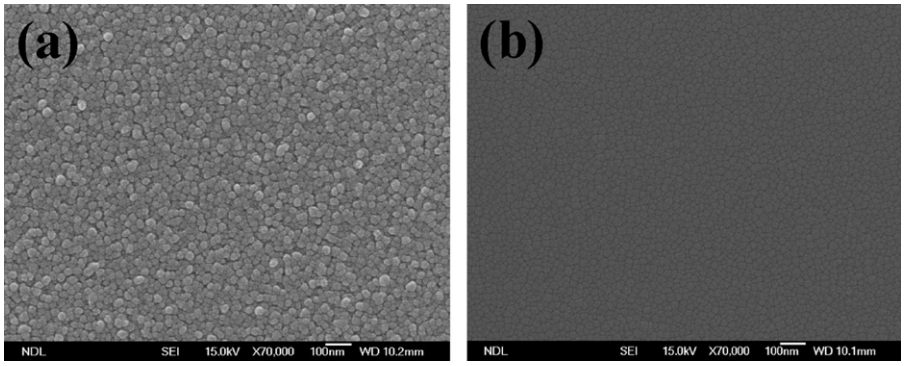

Fig. 5. SEM graphs of a-IGZO2 film (In:Ga:Zn = 1:1:1) with O_2 flow rates at (a) 0 and (b) 2 sccm, respectively.

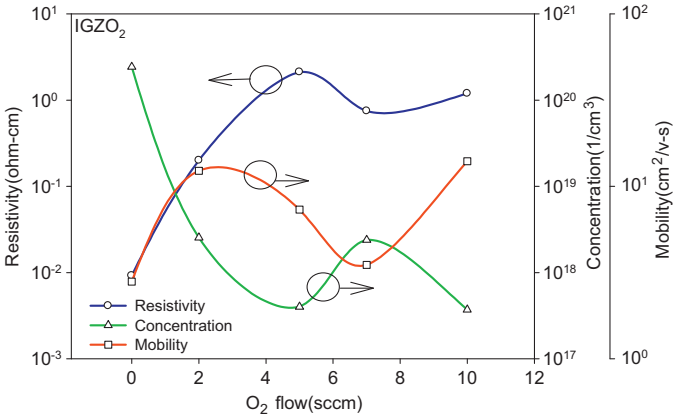

Fig. 6. Hall measurement plot of a-IGZO2 film (In:Ga:Zn = 1:1:1) as a function of O_2 flow rates with fixed Ar flow, 50 sccm.

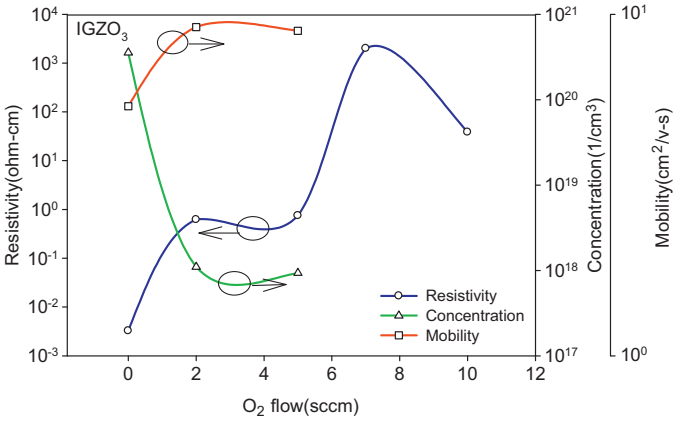

Fig. 7. Hall measurement plot of a-IGZO3 film (In:Ga:Zn = 1:1:2) as a function of O_2 flow rates with fixed Ar flow, 50 sccm.

condition (>5 sccm); finally, the carrier concentration decreased at the highest O_2 flow rate (>7 sccm). Increasing the atomic ratio of Zn in the IGZO ceramic target increased the capability of capturing O_2, leading to lower carrier concentration. Fig. 7 shows the Hall measurement plot of a-IGZO3 film (In:Ga:Zn = 1:1:2) as a function of O_2 flow rates with a fixed Ar flow equal to 50 sccm. The resistivity rose with the increasing O_2 flow and did not saturate when the O_2 flow rate was more than 5 sccm. Increasing the atom ratio of Zn in the IGZO ceramic target obviously increased the capability of capturing O_2, leading to lower carrier concentration ($<10^{18}$ cm^{-3}) at the O_2 flow rate equal to 5 sccm. Lower carrier concentration must be controlled at low levels to control TAOSs–TFT device characteristics with favorable stability and reproducibility. The resistivity of a-IGZO3 film at the highest O_2 flow rate (>7 sccm) was revealed to be more than 38.4 Ω cm, ascribed to the largest capability of capturing O_2. When the O_2 flow rate was zero, the results of a Hall measurement of a-IGZO films deposited from targets with a higher Zn atomic ratio showed lower resistivity, higher carrier concentration, and lower mobility.

4. Conclusions

To summarize a comparison of the XRD analyses of powder and Hall measurements of a-IGZO films suggests that increasing the zinc ion content, causes the main peaks (1 0 1) and (0 0 15) intensity of the respective $InGaZnO_4$ and $InGaZnO_6$ phases intensity, to increase in proportion to the conductivity and carrier concentration in a-IGZO films at O_2 flow rate equal to zero. The resistivity of a-IGZO film with a smaller ZnO atomic ratio saturated when the O_2 flow increases. Less content of Zn decreases the capability of O_2 capture. By increasing the O_2 flow rate, the carrier concentration decreases on the lower O_2 flow rate (<5 sccm), but the carrier concentration increases at the high O_2 flow rate condition (>5 sccm). Nevertheless, the resistivity of a-IGZO film with a higher Zn atomic ratio rises with the increasing O_2 flow and does not saturate when the O_2 flow rate is more than 5 sccm. Increasing the atomic ratio of ZnO in IGZO powder obviously increases the capability of capturing O_2, leading to higher resistivity and lower carrier concentration.

Acknowledgements

This work was supported by National Science Council Research Project (NSC 98-2218-E-159-002). Hall measurement and all others measurement were implemented in NCTU and National Nano Device Laboratory, Hsin-Chu, Taiwan, respectively. Authors also thanks for the proof reading this article from Wallace Academic Editing.

References

[1] K. Nomura, H. Ohta, A. Takagi, T. Kamiya, M. Hirano, H. Hosono, Room-temperature fabrication of transparent flexible thin-film transistors using amorphous oxide semiconductors, Nature 432 (2004) 488–492.

[2] H. Yabuta, M. Sano, K. Abe, T. Aiba, T. Den, H. Kumomi, K. Nomura, T. Kamiya, H. Hosono, High-mobility thin-film transistor with amorphous $InGaZnO_4$ channel fabricated by room temperature rf-magnetron sputtering, Applied Physics Letters 89 (2006), 112123- 1- 112123- 3.

[3] K. Nomura, A. Takagi, T. Kamiya, H. Ohta, M. Hirano, H. Hosono, Amorphous oxide semiconductors for high-performance flexible thin-film transistors, Japanese Journal of Applied Physics 45 (2006) 4303–4308.

[4] N.L. Dehuff, E.S. Kettenring, D. Hong, H.Q. Chiang, J.F. Wager, R.L. Hoffman, C.H. Park, D.A. Keszler, Transparent thin-film transistors with zinc indium oxide channel layer, Journal of Applied Physics 97 (2005), 064505- 1- 064505- 5.

[5] B. Yaglioglu, H.Y. Yeom, R. Beresford, D.C. Paine, High-mobility amorphous In_2O_3–10 wt% ZnO thin film transistors, Applied Physics Letters 89 (2006), 062103- 1- 062103- 3.

[6] R.L. Hoffman, Effects of channel stoichiometry and processing temperature on the electrical characteristics of zinc tin oxide thin-film transistors, Solid-State Electronics 50 (2006) 784–787.

[7] T. Miyasako, M. Senoo, E. Tokumitsu, Ferroelectric-gate thin-film transistors using indium-tin-oxide channel with large charge controllability, Applied Physics Letters 86 (2005), 162902- 1- 162902- 3.

[8] X.Q. Weia, Z. Zhanga, Y.X. Yub, B.Y. Manc, Comparative study on structural and optical properties of ZnO thin films prepared by PLD using ZnO powder target and ceramic targe, Optics & Laser Technology 41 (2009) 530–534.

[9] K.M. Krishna, M. Nisha, R. Reshmi, R. Manoj, A.S. Asha, M.K. Jayaraj, Electrical and optical properties of $ZnGa_2O_4$ thin film deposited by pulse laser deposition, Materials Forum 29 (2005) 243–247.

[10] M. Orita, M. Takeuchi, H. Sakai, H. Tanji, New transparent conductive oxides with $YbFe_2O_4$ structure, Japanese Journal of Applied Physics 34 (1995) L1550–L1552.

[11] Y.K. Moon, S. Lee, D.H. Kim, D.H. Lee, C.O. Jeong, J.W. Park, Application of DC magnetron sputtering to deposition of InGaZnO films for thin film transistor devices, Japanese Journal of Applied Physics 48 (2009) 031301–031304.